

*Supplement of*

**Rate coefficients for reactions of OH with aromatic and aliphatic volatile organic compounds determined by the Multivariate Relative Rate Technique**

**Jacob Shaw et al.**

Correspondence to: Jacob Shaw ([jacob.shaw@manchester.ac.uk](mailto:jacob.shaw@manchester.ac.uk))

**Table S1.** Measured  $k$  values and SAR derived  $k$  values for the reactions between OH and various aromatic and aliphatic VOCs studied.

Name	Measured $k / 10^{-12}$ $\text{cm}^3 \text{ molecule}^{-1} \text{ s}^{-1}$	SAR derived $k / 10^{-12} \text{ cm}^3 \text{ molecule}^{-1} \text{ s}^{-1}$	
		Jenkin et al. (2018a and 2018b)	Kwok and Atkinson (1995)*
<i>n</i> -butylbenzene	$11 \pm 4$	$7.6 \pm 1.1$	†
<i>n</i> -pentylbenzene	$7 \pm 2$	$8.7 \pm 1.3$	†
1,2-diethylbenzene	$14 \pm 4$	$14 \pm 2$	$8 \pm 4$
1,3-diethylbenzene	$22 \pm 4$	$21 \pm 3$	$13 \pm 7$
1,4-diethylbenzene	$16 \pm 4$	$14 \pm 2$	$8 \pm 4$
2-methylheptane	$9.1 \pm 0.3$	$7.8 \pm 1.2$	$8 \pm 4$
2-methylnonane	$11.0 \pm 0.3$	$11 \pm 2$	$11 \pm 6$
Ethylcyclohexane	$14.4 \pm 0.3$	$11 \pm 2$	$12 \pm 6$

\* see also Ziemann and Atkinson (2012)

† No electrophilic substituent constants ( $\sigma^+$ ) exist for either of the *n*-butyl or *n*-pentyl groups so this method was unable to derive a SAR value for these reactions.

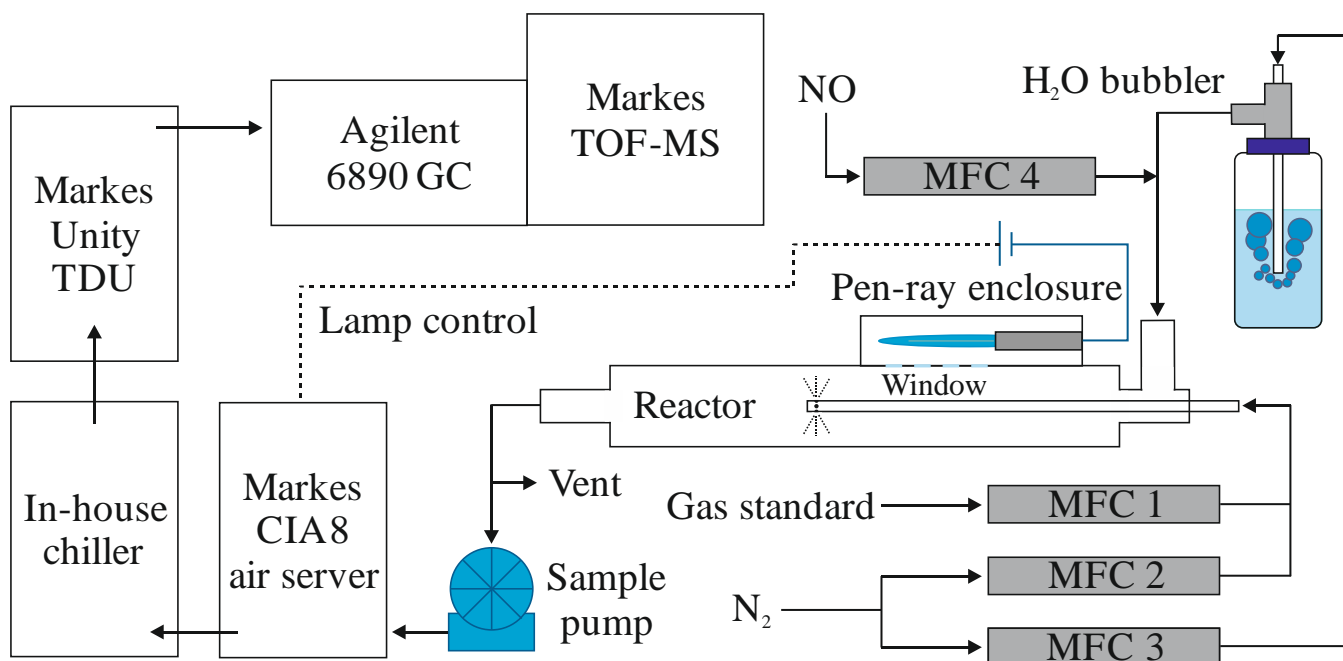


**Figure S1.** Schematic of the OH reactor configuration used. CIA8 is the air server and canister interface accessory; GC is the gas chromatograph; the MFCs are the mass flow controllers; TOF-MS is the time-of-flight mass spectrometer; TDU is the thermal desorption unit. The flow rate through MFC 1 was set to between 100 and 800 cm<sup>3</sup> min<sup>-1</sup>. The combined flow rate through MFC 1 and MFC 2 was kept at a constant 1750 cm<sup>3</sup> min<sup>-1</sup>. The flow rate through MFC 3, and hence through the H<sub>2</sub>O bubbler, was set to 1250 cm<sup>3</sup> min<sup>-1</sup>. The flow rate through MFC 4 was varied between 0 and 40 cm<sup>3</sup> min<sup>-1</sup>. This resulted in a total flow rate through the reactor of approximately 3000 cm<sup>3</sup> min<sup>-1</sup>. The residence time of VOC inside the reactor, after injection, was approximately 4 s, of which the oxidation chemistry is expected to occur in less than 0.5 s.

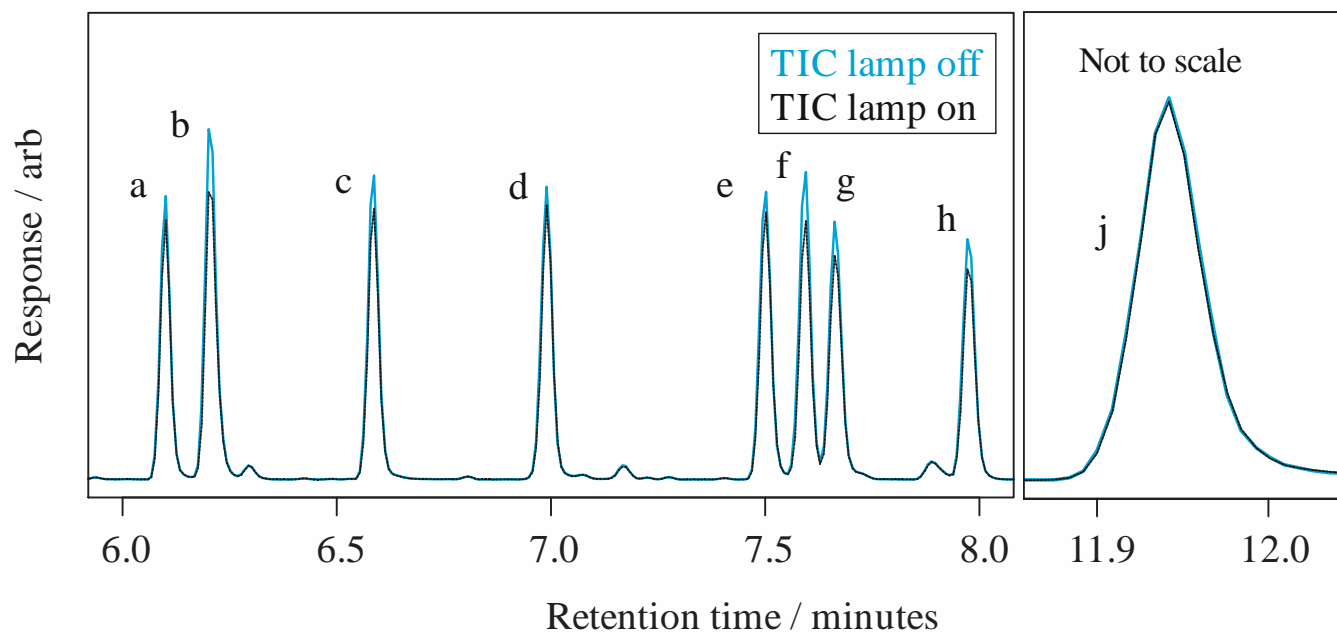


**Figure S2.** Typical total ion chromatogram (TIC) sections obtained for a ppbv mixing ratio gas standard (Mixture 1) with the lamp turned off (blue) and the lamp turned on (black). Greater differences in peak areas are observed for VOCs which react faster with OH. The peak assigned to *n*-pentylbenzene (shown on a different scale relative to the others) had no reduction in peak area for lamp-on samples relative to lamp-off samples. The peaks can be assigned as follows, with their evaluated literature rate coefficients for reaction with OH provided in brackets (in units of  $10^{-12} \text{ cm}^3 \text{ molecule}^{-1} \text{ s}^{-1}$ ): a, ethylbenzene ( $7.0 \pm 2$ ); b, *m*-xylene ( $23 \pm 3$ ); c, *o*-xylene ( $13 \pm 3$ ); d, isopropylbenzene ( $6.3 \pm 2$ ); e, *n*-propylbenzene ( $5.8 \pm 1.5$ ); f, 3-ethyltoluene ( $19 \pm 7$ ); g, 4-ethyltoluene ( $12 \pm 4$ ); h, 2-ethyltoluene ( $12 \pm 4$ ); j, *n*-pentylbenzene, (n/a).

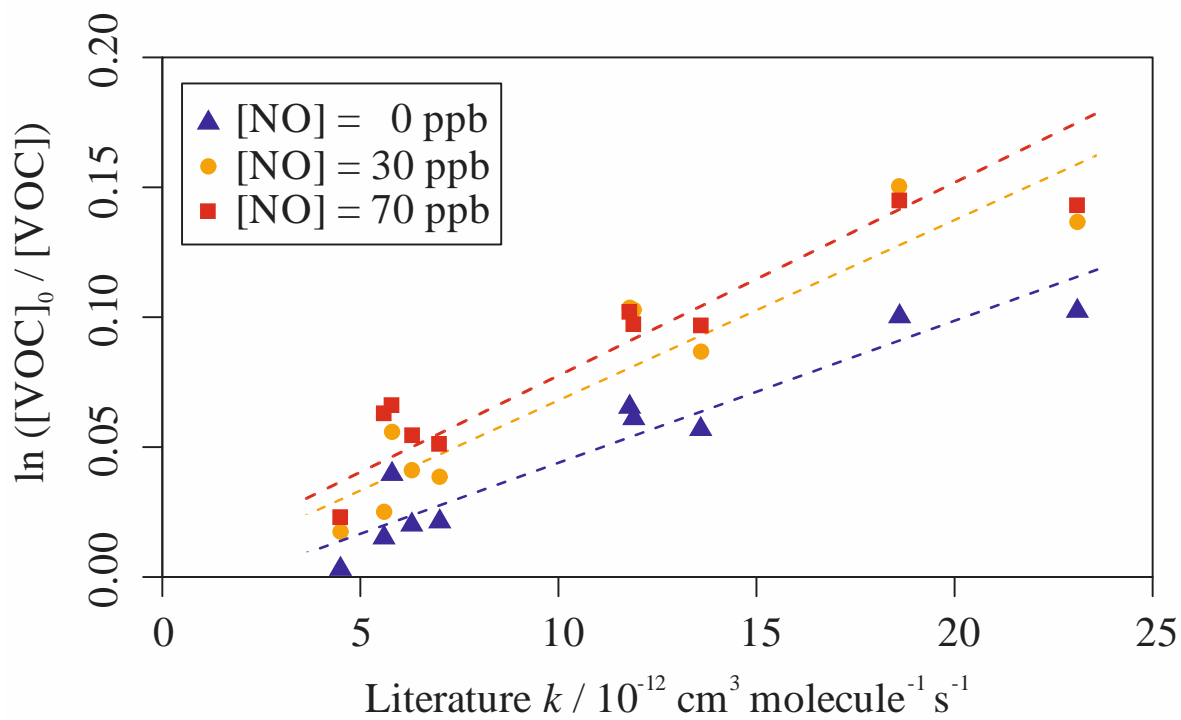


**Figure S3.** Relative rate plots for Mixture 1 (OH reactivity of  $18 \text{ s}^{-1}$ ) with NO concentrations of 0, 30 and 70 ppbv at  $296 (\pm 2) \text{ K}$ . The calculated  $OH_{exp}$  was equal to  $5.5 (\pm 0.6)$ ,  $6.9 (\pm 0.9)$  and  $7.5 (\pm 0.8) \times 10^9 \text{ molecules cm}^{-3} \text{ s}$  respectively. The  $R^2$  values for the weighted linear fits were 0.899, 0.853 and 0.909 for [NO] = 0, 30 and 70 ppbv respectively.

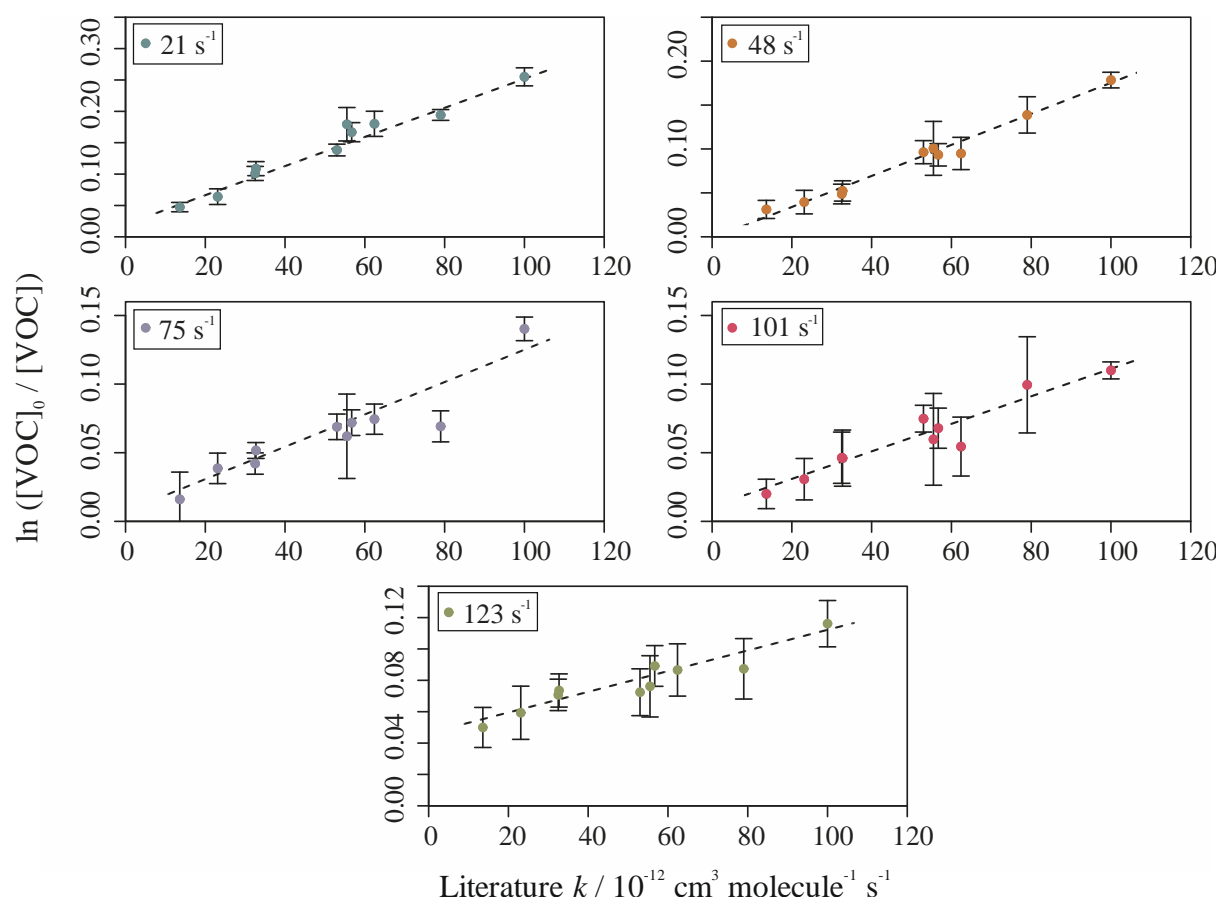


**Figure S4.** Relative rate plots for Mixture 3 with OH reactivities of 21, 48, 75, 101 and 123  $\text{s}^{-1}$ . The  $R^2$  for the weighted linear fits were 0.958, 0.980, 0.907, 0.967 and 0.829 respectively. The values of  $OH_{exp}$  were  $2.3 (\pm 0.1)$ ,  $1.8 (\pm 0.1)$ ,  $1.2 (\pm 0.2)$ ,  $1.0 (\pm 0.1)$  and  $0.7 (\pm 0.1) \times 10^9$  molecules  $\text{cm}^{-3} \text{s}$  respectively.

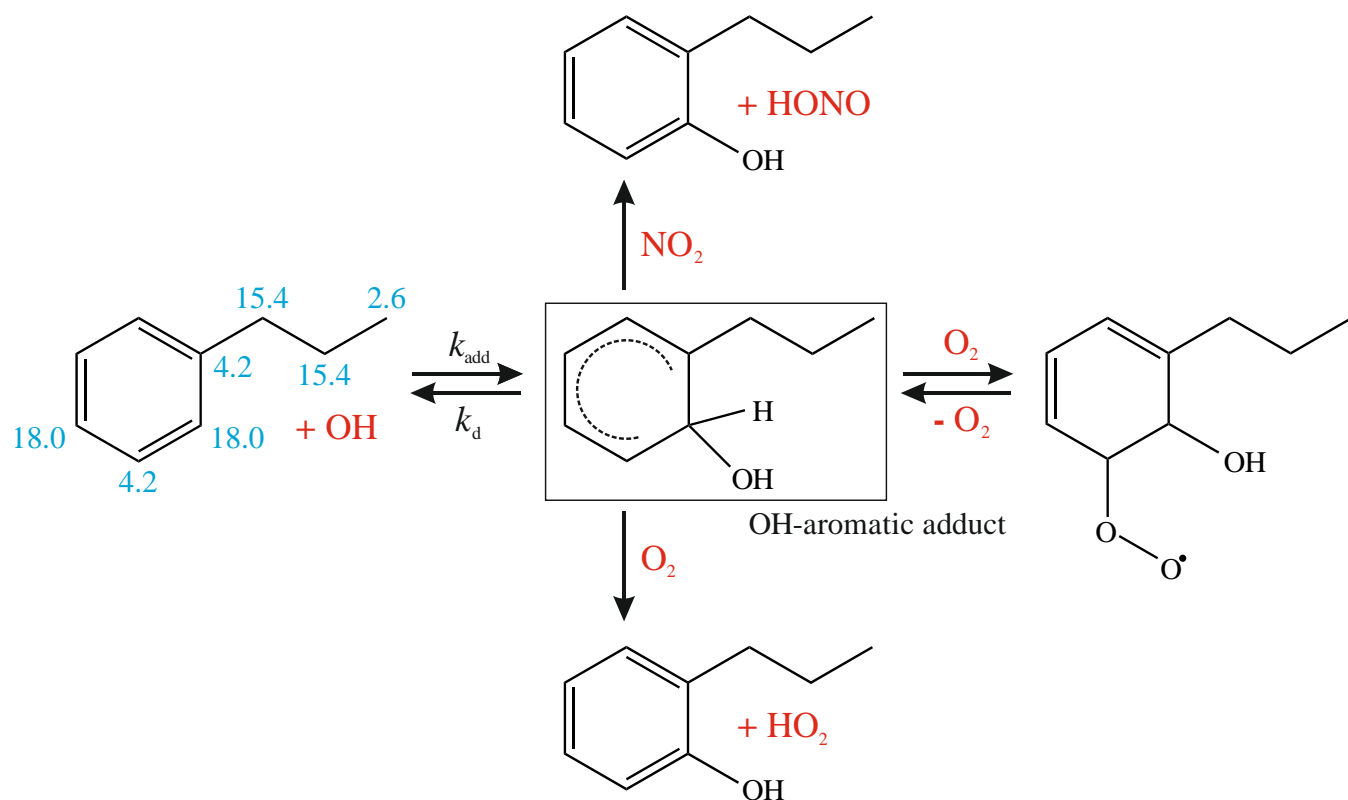


**Figure S5.** Example schematic for the OH oxidation of *n*-propylbenzene through OH-addition to the aromatic ring. Pathways due to H-abstraction from the substituent are not shown. Branching ratios (for all OH reaction pathways; see Jenkin et al. (2018a)) are indicated in blue, with OH-addition at the *ortho*- and *para*- position representing the largest probabilities. The path defined as  $k_{\text{add}}$  results in the formation of the OH-aromatic adduct. Back decomposition ( $k_{\text{d}}$ ) can result in the reformation of the original aromatic species unless further reaction, with either of  $\text{O}_2$  or  $\text{NO}_2$ , can take place.

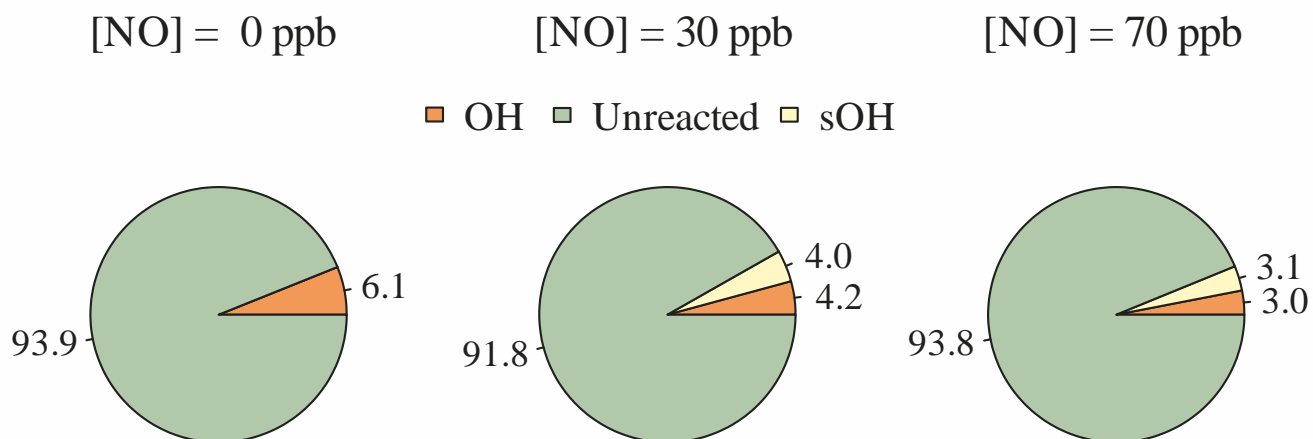


**Figure S6.** Simulated impact of different initial [NO] on the total VOC sink. Most of the VOCs remained unreacted in all three scenarios; the extent of the unreacted proportion varied from VOC to VOC depending on the rate at which that VOC reacted with OH. The VOCs were most depleted when [NO] was set to 30 ppb in the reactor.